LA-UR-73-1180

Conf-730823--19

TITLE: FISSION AND COMPLETE FUSION MEASUREMENTS IN ^{40}Ar BOMBARDMENTS OF ^{58}Ni AND ^{109}Ag

AUTHOR(S): H. Gutbrod, G.S.I.Darmstadt, German
F. Plasil, ORNL
H. C. Britt, P-DOR
B. H. Erkkila, P-12
R. H. Stokes, P-12
M. Glann, Univ. of Rochester

SUBMITTED TO: Proceedings of the IAEA Symposium on Physics and Chemistry of Fission.

Los Alamos Scientific Laboratory
of the University of California
LOS ALAMOS, NEW MEXICO 87544

Form No. 836
St. No. 2629
1/73

UNITED STATES
ATOMIC ENERGY COMMISSION
CONTRACT W-7405-ENG. 36

FISSION AND COMPLETE FUSION MEASUREMENTS IN ^{40}Ar BOMBARDMENTS OF ^{58}Ni AND ^{109}Ag*

H.H. Gutbrod
G.S.I. Darmstadt, Germany
F. Plasil
Oak Ridge National Laboratory, Oak Ridge, Tenn.
H.C. Britt, B.H. Erkkila, and R.H. Stokes
Los Alamos Scientific Laboratory, Los Alamos, New Mexico
M. Blann
University of Rochester, Rochester, New York

ABSTRACT

Thin targets of ^{58}Ni and ^{109}Ag have been bombarded with 197 and 288 MeV ^{40}Ar ions from the Berkeley SUPER-HILAC. A particle telescope consisting of a gas proportional ΔE counter and a silicon surface barrier E detector was used to measure all reaction products ranging from elastically scattered argon ions to compound nucleus evaporation products. Fission fragments and transfer products were also detected. A good separation between fission fragments and other reaction products was possible in the case of the ^{109}Ag + ^{40}Ar reaction. Angular distributions were obtained from 4° to 40° in the laboratory system. Elastic scattering and a ^{252}Cf source were used to obtain energy and angular calibrations.

The fission fragment angular distribution is characterized by a 1/sinθ function, and the integrated fission cross-section was found to be 300 and 600 mb for Ar + Ag at 197 and 288 MeV.

*Work supported in part by the U.S. Atomic Energy Commission and Gesellschaft für Schwerionenforschung MBH.

Results have been interpreted in terms of a model in which fission competes with other modes of de-excitation of the compound nucleus, and in which the effects of angular momentum on the fission barrier are taken into account. The implications of this conclusion are discussed. Comparisons are also made with models for the complete fusion cross section which are based on the contact configuration for the interacting two body systems.

FISSION AND COMPLETE FUSION MEASUREMENTS IN ^{40}Ar BOMBARDMENTS OF ^{58}Ni AND ^{109}Ag*

H.H. Gutbrod
G.S.I. Darmstadt, Germany
F. Plasil
Oak Ridge National Laboratory, Oak Ridge, Tenn.
H.C. Britt, B.H. Erkkila, and R.H. Stokes
Los Alamos Scientific Laboratory, Los Alamos, New Mexico
M. Blann
University of Rochester, Rochester, New York

1. INTRODUCTION

The work to be discussed is part of a broad program to measure as many of the main reaction channels as possible for heavy ion induced reactions. It is planned ultimately to do this for a number of target and projectile combinations, in the hope that these results will help provide the proving grounds for various macroscopic models of heavy ion reactions.

The systems to be discussed are ^{40}Ar induced reactions on targets of ^{58}Ni and ^{109}Ag at incident energies of 197 and 288 MeV. Beams were obtained from the Berkeley Superhiluc. We will describe the experimental method used, the method of analyzing the data, and the results which consist of cross sections for compound nucleus evaporation products (evaporation residues), fission cross sections and angular distributions, a fission mass-yield distribution, and fission fragment kinetic energy distributions. Results will then be compared with several models which predict angular momentum limits for either the compound nucleus formation cross section or for the evaporation residue cross section.

---

*Work supported in part by the U.S. Atomic Energy Commission and Gesellschaft für Schwerionenforschung MBH.

2. EXPERIMENTAL METHOD

The results to be reported were obtained from angular distributions of reaction products measured with a gas-solid state ΔE-E counter telescope[1] with a ΔE thickness of ∿250μg/cm². Targets were ≤200μg/cm². Line targets on carbon backing were used for all measurements except the 197 MeV results in ^{109}Ag and the angular correlation result at 288 MeV. A self-supporting target was used for the latter. A contour plot of two spectra is shown as an example in fig. 1 (see caption). Energy resolution was ∿0.5% in the E plane and ∿6% in ΔE. The features to be noted in fig. 1 are the elastic scattering peak, the evaporation residue distribution, a fission-like distribution, and in some spectra a distribution which has been attributed to carbon backings or carbon target buildup. The latter is not evident in the examples of fig. 1. Low Z yields may also be seen in the contour from the ^{58}Ni target. Elastic scattering and use of ^{252}Cf sources were used in the calibration of the ΔE and E scales.

Evaporation residue cross sections have been obtained by integration over angle of the cross sections from distributions such as shown in this example; fission angular distributions were obtained by integration of the fission-like products. The mass yield to be shown was deduced from the Z distribution of the fission-like fragments from a long run at 40° Lab; the kinetic energy distribution also was obtained from this run. Range energy results (dE/dX) due to Northcliffe and Schilling were used in identifying product atomic numbers[2]. Fission cross sections were obtained from the angular distributions of the fission-like group and at 288 MeV ^{40}Ar + ^{109}Ag, a cross section was also obtained from a measurement of the angular correlation of the two fragments.

3. RESULTS

Angular distributions for the evaporation residues are shown in fig. 2. These results were integrated to get total cross sections. The largest source of error is thought to be the extrapolation of the measured distributions to 0°; total errors from all sources are believed to be ≤15%. Uncertainties in the extrapolation are reduced by the sinθ factor which enters into the integration of the distributions of fig. 2. Results for fusion and fission cross sections are summarized in Table I. Angular distributions of fission-like products are shown in fig. 3. Transformation to CM was made assuming symmetric binary fission. A 1/sinθ curve was fitted to the experimental results, and is shown as the solid line on this figure. Fission cross sections were based on integration of the 1/sinθ distribution, corrected for the fraction of the mass yield estimated to be missing from the integration of each spectrum. This results in a very large uncertainty for the ^{40}Ar + ^{58}Ni system since the carbon backing made it undesirable to integrate below Z 22. The experimental results at 288 MeV on ^{109}Ag show some evidence of being more forward peaked than the $1/\sin\theta$ distribution. It is not clear if this is a statistically significant deviation. If it is, it could imply a contribution to the fission cross section from a non-equilibrium system.

The charge yield deduced from the ΔE identification for the system ^{109}Ag + ^{40}Ar at 288 MeV is shown in fig. 4. The distribution is centered at $\sim Z=30$, which is consistent with the expectation for symmetric fission followed by particle evaporation. The mass yield implied by these results has FWHM of $\sim$40 AMU. Spectra were not integrated below $Z=22$ when fig. 4 was prepared. Preliminary results indicate a distribution which is somewhat skewed to lower masses. Kinetic energy distributions for the light, medium and heavy fragments are shown in fig. 5. The shift to higher energies for lower mass in a manner consistent with binary fission may be seen. A fission correlation experiment was also performed during the run on which these data are based. The E counter used in the correlation subtended an angle of ±7.5°, which was estimated to record 47% of binary coincidence events. With the telescope at +40°, the E counter was placed at -57.5° giving a correlation angle of 97.5°. This may be compared with a predicted value of 101° for symmetric binary fission. The cross section obtained in this measurement also agreed well with estimates from the singles measurements.

4. DISCUSSION

Experimental results of this work are compared with predicted angular momentum limits in fig. 6. The experimental evaporation residue cross sections are shown, and for the ^{109}Ag targets, the sum of evaporation residue plus fission cross sections are also indicated. The results show that at the higher energy in the Ar + Ag case, the sum of evaporation residue and fission cross sections are still considerably less than the expected total reaction cross section.

The lower solid curve is the predicted limit to the evaporation residue cross sections due to application of the rotating liquid drop model[2]. The fission barriers and ground state rotational energies have been computed as a function of angular momentum by Cohen *et al*[3]. These values were used in a Bohr-Wheeler[4] type fission-evaporation competition calculation for each impact parameter for ^{40}Ar + ^{109}Ag. Multiple particle emission and multiple chance fission were included in the calculation[5]. This calculation should predict the cross section of the evaporation residue if the compound nucleus is actually formed with partial waves higher than those which give highly fissionable nuclei. The comparison between calculated and experimental results in fig. 6 is quite satisfactory.

Models have been formulated to predict the angular momentum limits for the formation of a compound nucleus based on the potential energy surface for the initial contact configuration, or for related shapes.[6-9] These treatments are similar to one another in that they consider the surface attractive and Coulomb plus centrifugal repulsive terms in computing the potential energy.

The first such treatment to our knowledge was due to Kalinkin and Petkov[6], who considered ellipsoidal contact shapes. More recently Wilczynski has calculated the result for a configuration of spherical target and projectile systems undergoing a grazing-like collision.[7] The predicted limit to the compound nucleus formation cross section due to Wilczynski's formulation is shown by the lower dotted curve of fig. 6. If the experimentally observed fission yield results from fission of a compound nucleus, then the calculation with Wilczynski's model should be compared with the sum of fission plus evaporation residue cross sections. In this case, Wilczynski's result seriously underestimates the fusion cross section at 288 MeV ^{40}Ar + ^{109}Ag.

Tsang and Swiatecki are considering the problem of compound nucleus formation in a dynamic model with frictional effects, based also on a contact configuration for two spheres.[8] Their limits to the compound nucleus formation cross section when the nuclear viscosity is high are shown as the upper dotted curve of fig. 6. A similar result follows from a related and in some ways similar treatment due to R. Bass.[9] The agreement between the limits of the Tsang-Swiatecki treatment and the experimental fission plus evaporation residue cross section may be a preliminary indication of high nuclear viscosity for heavy ion reactions in the energy range of these results.

5. CONCLUSIONS

The data discussed indicate that far less than the full reaction cross sections are found in the evaporation residues. The evaporation residue cross sections are in reasonably good agreement with values predicted by the rotating liquid drop model with fission competition, but the actual fission cross sections can be much less than the difference between calculated evaporation residue and total reaction cross sections. Presumably the difference is to be found in direct reaction products, and evidence has been found for high transfer cross sections at 288 MeV in γ-ray activation studies of ^{40}Ar + ^{109}Ag.[10] For the case Ag + Ar, the cross section for the evaporation residue and fission is consistent with the predictions of a model based on the contact configuration with high friction as formulated by Tsang and Swiatecki. The fission product angular distributions are generally consistent with a $1/\sin\theta$ function, consistent with at least a major portion of the fission cross section being due to equilibrium fission.

6. ACKNOWLEDGMENTS

The authors wish to express their appreciation to Dr. A. Chiorso and the entire operating crew of the Berkeley Heavy Ion Accelerator. The programming assistance of Dr. R. Epple is similarly very much appreciated. We wish to thank Mrs. J. Gursky for preparing the targets. We have very much enjoyed helpful discussions with Drs. H. Krappe, W. D. Meyers, W. J. Swiatecki and C. F. Tsang.

REFERENCES

[1] K.D. HILDENBRAND, H.H. GUTBROD, W.V. OERTZEN and R. BOCK, Nucl. Phys. A157(1970)297.

[2] L.C. NORTHCLIFFE and R.F. SCHILLING, Nucl. Data Tables 7, No.3-4(1970).

[3] S. COHEN, F. PLASIL, and W.J. SWIATECKI, LBL Preprint LBL-1502(1972) submitted to Annals of Physics; Proceedings of the Third Conference on Reactions Between Complex Nuclei(ed. by A. GHIORSO, R.M. DIAMOND and H.E. CONZETT) Univ. of Calif. Press, Berkeley(1963) 325.

[4] N. BOHR and J.A. WHEELER, Phys. Rev. 56(1939)426.

[5] M. BLANN and F. PLASIL, Phys. Rev. Lett. 24(1972)303.

[6] B.N. KALINKIN and I.Z. PETKOV, Acta. Phys. Polon. 25(1964)265.

[7] J. WILCZYNSKI "Calculations of the critical angular momentum in the entrance channel", Niels Bohr Institute Preprint(1973) unpublished.

[8] C-F. TSANG and W.J. SWIATECKI, private communication (1973).

[9] R. BASS, private communication(1973).

[10] M.E. HILLE, P. HILLE, and H.H. GUTBROD, private communication(1973).

Table 1: Summary of cross sections from ^{40}Ar bombardment

Target	^{40}Ar Energy (MeV-Lab)	cross sections (mb) Evaporation Residue	Fission
^{58}Ni	288	900±120	
	197	880±120	(400±150)[a]
^{109}Ag	288	670±100	600±90
	197	620±90	300±45

a) Rough estimate based on integration of less that half the mass-yield distribution.

FIGURE CAPTIONS

Fig. 1 Contour plots of counter-telescope data from ^{40}Ar (197MeV) on ^{58}Ni and ^{109}Ag targets. The laboratory angles were 10° and 12° respectively. The ordinate is the logarithm of the number of counts. The high peaks at low ΔE and high E are the elastic ^{40}Ar peaks. A ridge due to inelastic events and slit scattered ^{40}Ar may be seen at energies below the elastic peak. The peaks at high ΔE and relatively low E are the evaporation residues, and the group at medium E with a broad distribution in ΔE is the fission like group.

Fig. 2 Angular distributions of evaporation residues following ^{40}Ar bombardment of ^{58}Ni, ^{92}Mo, and ^{109}Ag targets. The ordinate is broken to allow a double display. The solid line was drawn visually through the points before integration over angle. The dotted lines represent one set of extrapolations to 0°. Squares, triangles, and circles represent the experimental measurements.

Fig. 3 Angular distributions of fission like products. Points represent experimental measurements converted to CM assuming symmetric binary fission. Solid lines are best fit results of a 1/sinθ curve. For ^{40}Ar + ^{58}Ni the evaporation residue angular distribution is shown for comparison as a dashed curve.

Fig. 4 Charge distribution curve deduced from ΔE of fission like products measured at 40° lab. The open points represent the experimental results converted to CM and integrated assuming a 1/sinθ angular distribution. The solid curve was arbitrarily drawn, and has been shown as a dashed curve below Z = 24 where it is extrapolated.

Fig. 5 Kinetic energy distribution of fragments measured at 40°. The ordinate is number of counts, the abscissa is kinetic energy in the laboratory system. Counts from several Z were combined for statistical purposes. The peaks at low energy are tho ght to result from heavy transfer products which give a dE/dX similar to low energy fission fragments. Those events were not included in the integrations of fig. 4.

Fig. 6 Cross sections versus ^{40}Ar energy. The heavy solid curve represents a calculated total reaction cross section. Open points represent the experimentally measured evaporation residue cross sections. Solid points represent the sum of measured fission plus evaporation residue cross sections. The thin solid curves are calculated evaporation residue yields based on fission competition with a rotating liquid drop. The lower dotted curve represents predicted complete fusion yields due to Wilczynski's formulation based on contact configuration. The upper dotted curve represents the authors interpretation of the limit due to a formulation of Tsang and Swiatecki, and also of Bass.

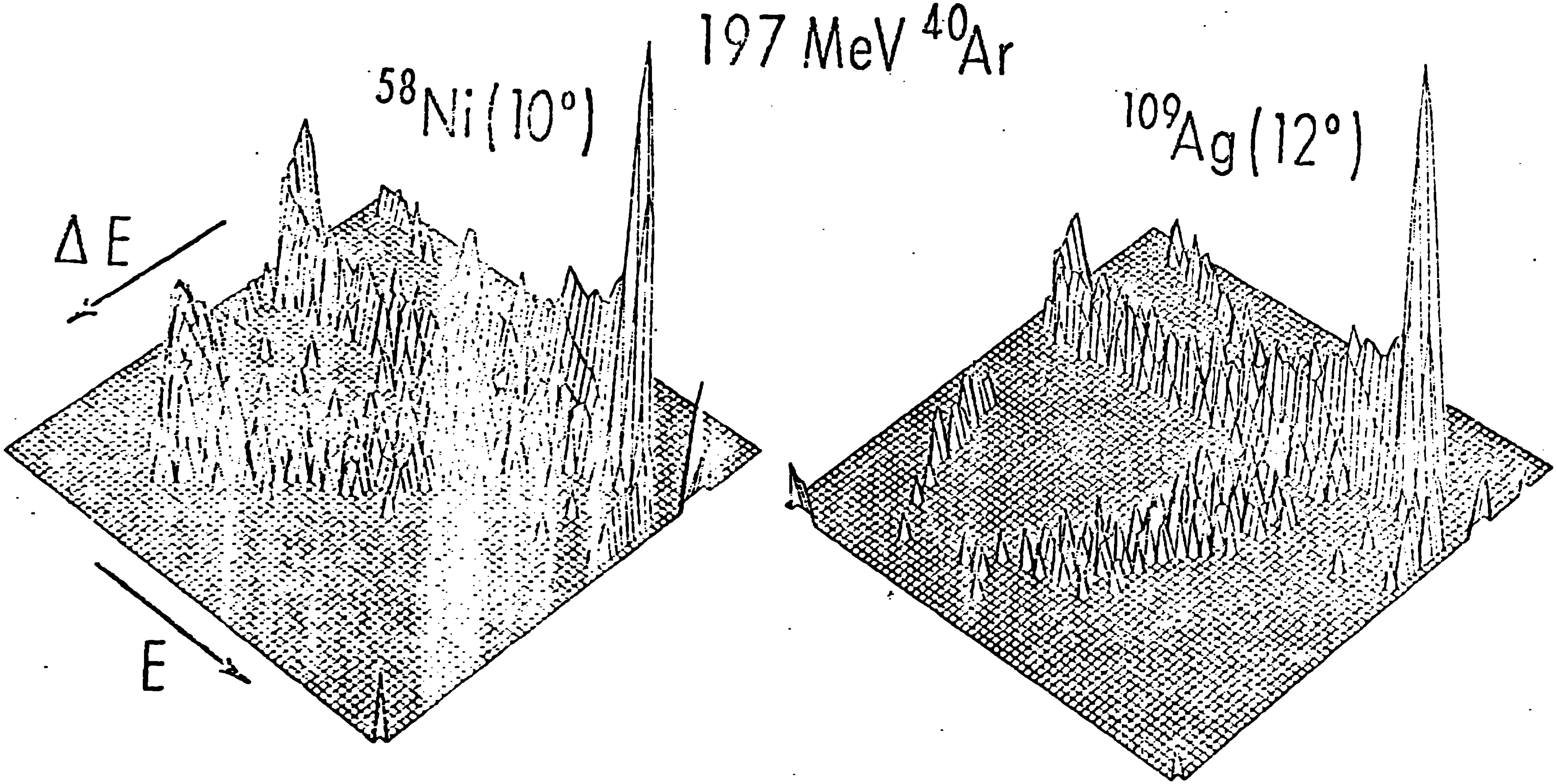
197 MeV 40Ar
58Ni(10°)
109Ag(12°)
ΔE
E

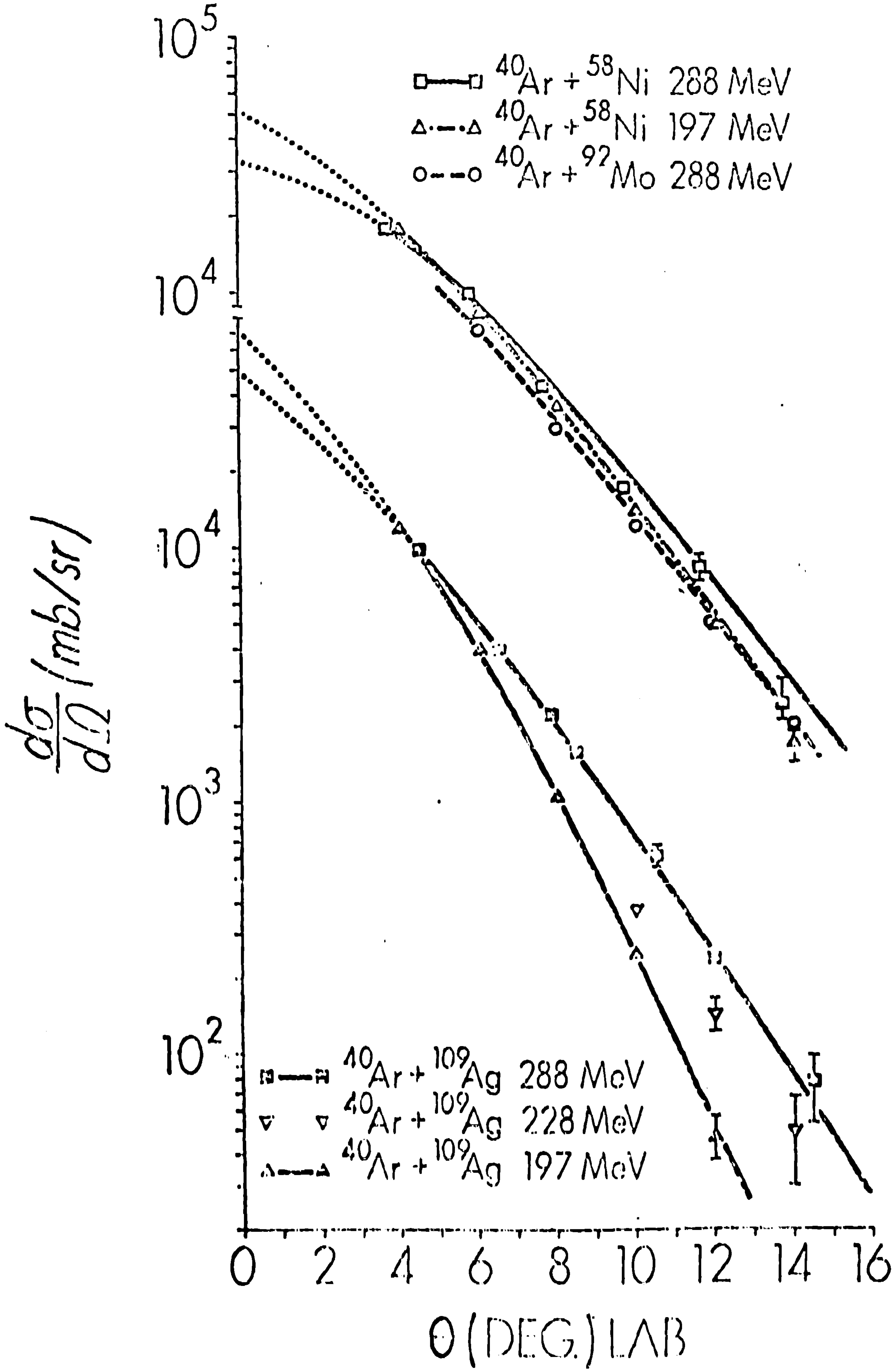

$^{40}Ar + ^{58}Ni$ 288 MeV
$^{40}Ar + ^{58}Ni$ 197 MeV
$^{40}Ar + ^{92}Mo$ 288 MeV
$^{40}Ar + ^{109}Ag$ 288 MeV
$^{40}Ar + ^{109}Ag$ 228 MeV
$^{40}Ar + ^{109}Ag$ 197 MeV
10^5
10^4
10^4
10^3
10^2
$\frac{d\sigma}{d\Omega}$ (mb/sr)
0 2 4 6 8 10 12 14 16
θ (DEG.) LAB

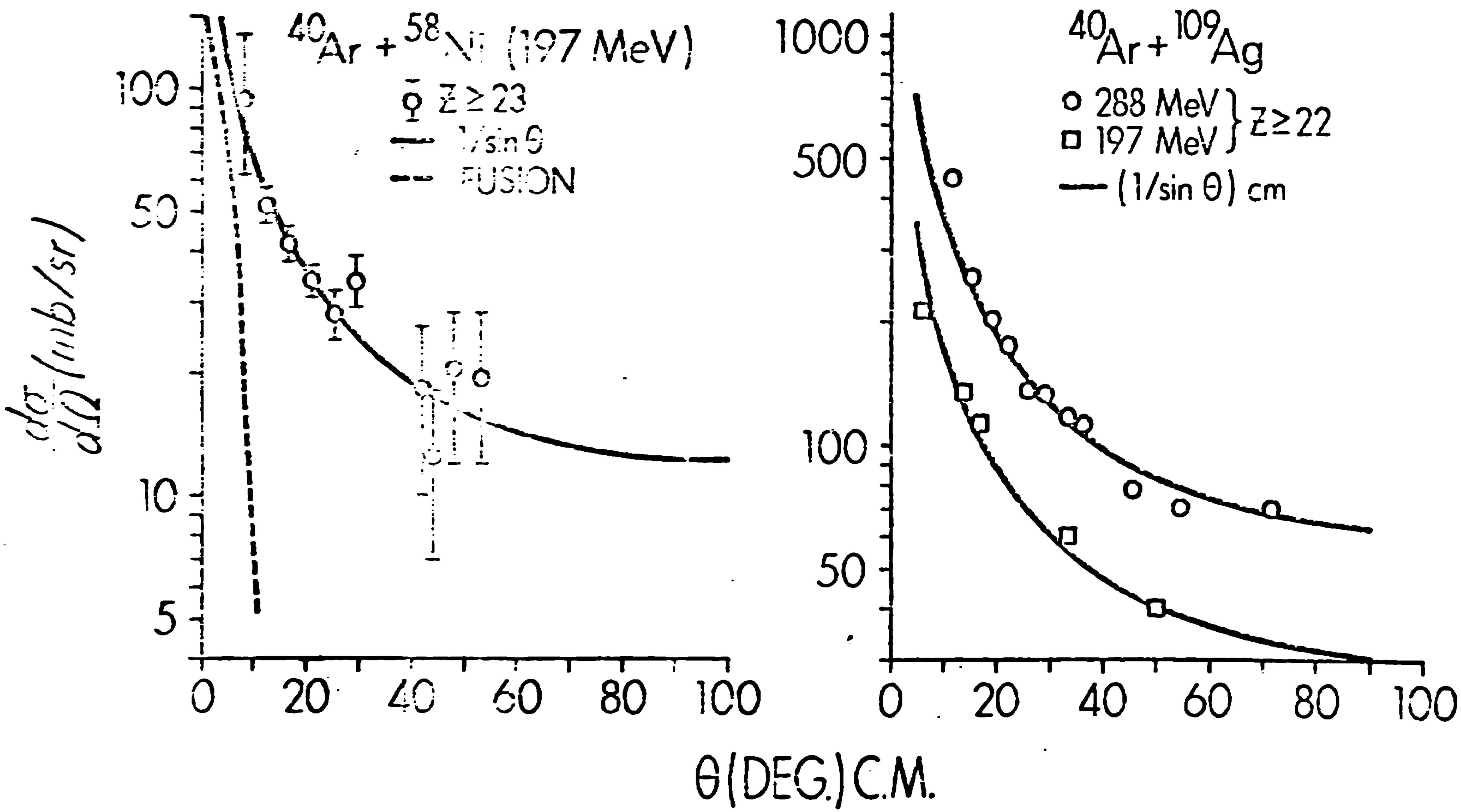

$^{40}Ar + ^{58}Ni$ (197 MeV)
Z ≥ 23
1/sin θ
FUSION
$\frac{d\sigma}{d\Omega}$ (mb/sr)
$^{40}Ar + ^{109}Ag$
288 MeV
197 MeV
Z ≥ 22
(1/sin θ) cm
θ (DEG.) C.M.

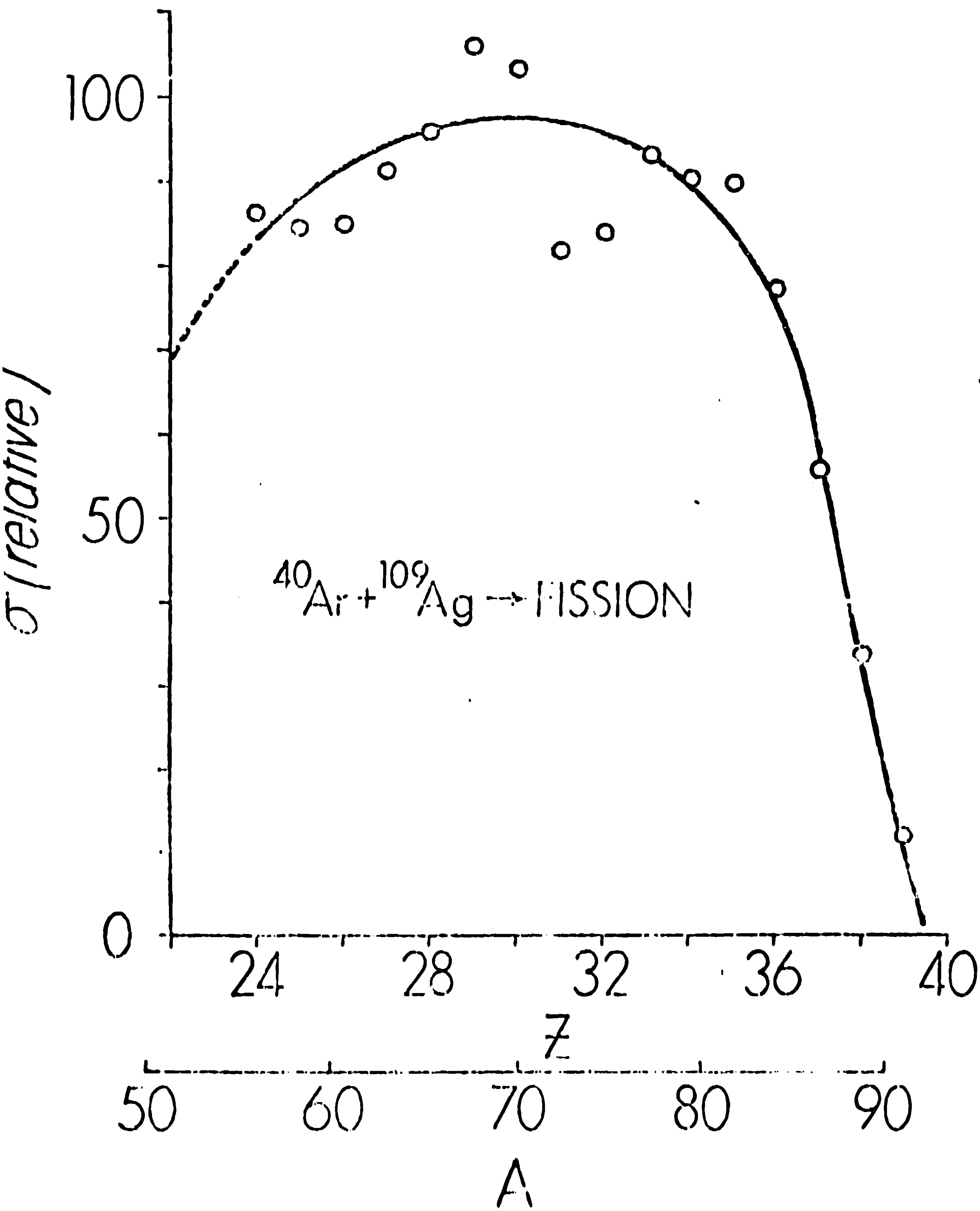

100
50
0
σ (relative)
$^{40}Ar + ^{109}Ag \to$ FISSION
24
28
32
36
40
Z
50
60
70
80
90
A

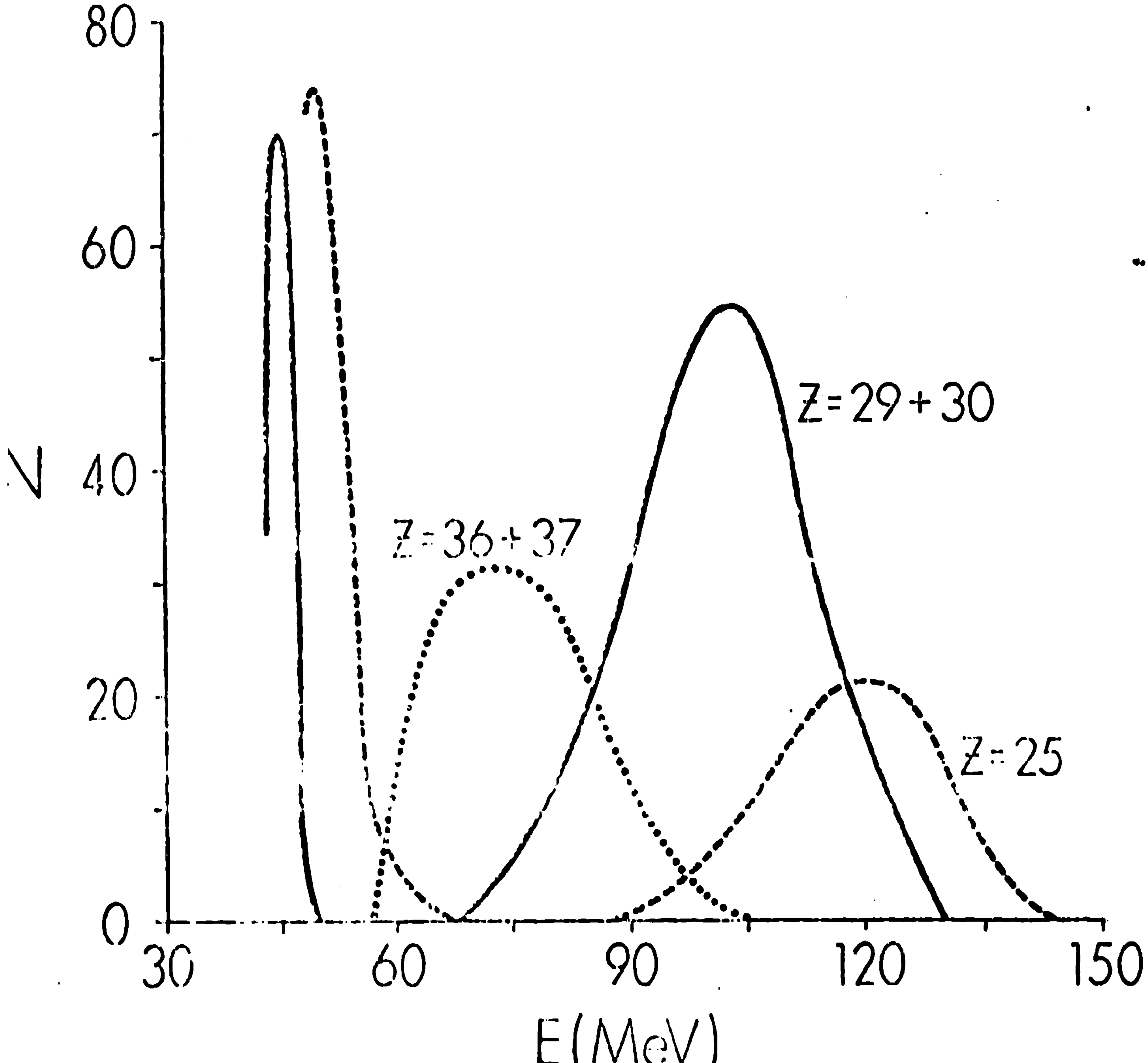

80
60
40
20
0
N
Z=29+30
Z=36+37
Z=25
30
60
90
120
150
E(MeV)

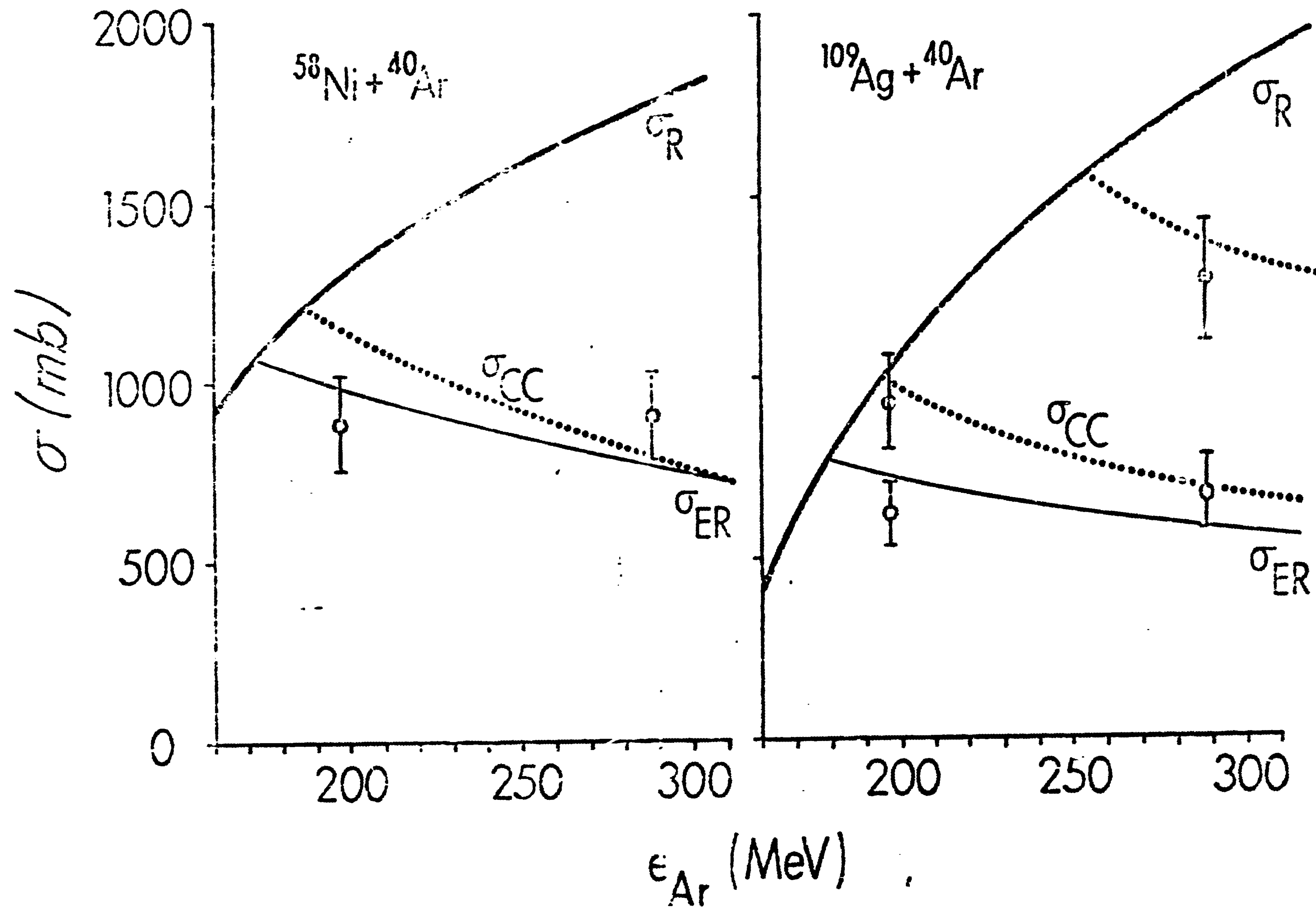

$^{58}Ni + ^{40}Ar$
$^{109}Ag + ^{40}Ar$
σ_R
σ_{CC}
σ_{ER}
σ (mb)
2000
1500
1000
500
0
200
250
300
ϵ_{Ar} (MeV)